# Radiation Characteristics of Circular Microstrip Patch Antenna with and Without Air Gap Using Neuro-Spectral Computation Approach

SAMI BEDRA, RANDA BEDRA
Department of Electronics.
University of Batna.
Batna, 05000 Batna.
Algeria.
bedra_sami@hotmail.fr

*Abstract:* - In this paper, we propose an artificial neural network (ANN) in conjunction with spectral domain formulation for fast and accurate determination of the resonant frequency and bandwidth of circular microstrip antenna with and without air gap. This neurospectral approach reduces the problem complexity. The results obtained from the neural model are in very good agreement with the experimental results available in the literature. Finally, numerical results for the air gap tuning effect on the resonant frequency and bandwidth of circular microstrip structure are also presented.

*Key-Words:* - Circular microstrip antenna; artificial neural network; spectral analysis; tunable structure.

## 1 Introduction

The increase in complexity of device modeling has led to rapid growth in the computational modeling research arena. To accommodate computational complexity, several computer aided design (CAD) modeling engines such as artificial neural networks (ANNs) were used [1-5] ANNs, emulators of biological neural networks, have emerged as intelligent and powerful tools and have been widely used in signal processing, pattern recognition, and several other applications [3-4]. ANN is a massively parallel and distributed system traditionally used to solve problems of nonlinear computing [5].

The MSA is an excellent radiator for many applications such as mobile antenna, aircraft and ship antennas, remote sensing, missiles and satellite communications [6]. It consists of radiating elements (patches) photo etched on the dielectric substrate. Microstrip antennas are low profile conformal configurations. They are lightweight, simple and inexpensive, most suited for aerospace and mobile communication. Their low power handling capability posits these antennas better in low power transmission and receiving applications [7]. The flexibility of the Microstrip antenna to shape it in multiple ways, like square, rectangular, circular, elliptical, triangular shapes etc., is an added property. The resonant frequency value of a microstrip patch antenna depends on the structural parameters, and it is evident that if the resonant frequency is to be changed, a new antenna is needed. In order to achieve tunable resonant frequency characteristic, an adjustable air gap layer can be inserted between the ground plane and substrate, resulting in a two-layer structure. Using the magnetic wall cavity model, some efforts have been made to analyze microstrip antennas with air gaps [8-16]. Since the cavity model [8-13] do not consider rigorously the effects of surface waves and fringing fields at the edge of the patch [15], and cannot be used to deal with multilayered structures, the moment method in Hankel transform domain [14, 15], provides better accuracy but its computational cost is high due to the evaluation of the slowly decaying integrals and the iterative nature of the solution process. Even though all the losses can be directly included in the analysis, produced results may not provide satisfactory accuracy for all the cases. Because of these problems, Mishra and Patnaik have introduced the use of neural networks in conjunction with spectral domain approach to calculate the complex resonant frequency [17] and the input impedance [18] of rectangular microstrip resonators, this approach is named the neurospectral method. In reference [17], the computational complexity involved in finding complex root is reduced, whereas, in reference [18], the neural network method evaluates the integrals appearing in the matrix impedance. Later on [19], Mishra and Patnaik have demonstrated the force of the neurosperctal approach in patch antenna design by using the reverse modeling to determine the patch length for a given set of other parameters.

In this paper, we develop fast and accurate model based on ANN technique to calculate the resonant frequencies of circular microstrip antennas. ANN is used to model the relationship between the parameters of the microstrip antenna and the resonant frequencies obtained from the spectral domain approach. This relatively simple model allows designers to predict accurately the resonant frequencies for a given design without having to develop or run the spectral method codes themselves. With the increase of design parameter's number, the network size increases, resulting in an increase in the size of training set required for proper generalization. Because of the different natures of the additional parameters, data generation becomes more complicated, a solution to this problem seems necessary. Electromagnetic knowledge [15] combined with artificial neural network are proposed here to solve this problem.
The aim of this work is to determine effective dielectric constant and height for the substrate using electromagnetic knowledge and then we use these effective parameters in the dyadic Green's function of two-layer structure (see Fig. 1). The resulting values are close to those computed using the Green's dyad. The different network input and output parameters are shown in Fig. 2. It is clear from this figure that although an air gap substrate is considered, only three inputs are needed.

## 2 Spectral Domain Formulation

The patch is assumed to be located on a grounded dielectric slab of infinite extent, and the ground plane is assumed to be perfect electric conductor. The circular patch with radius $a$ is printed on a substrate with dielectric constant, $\varepsilon_r$ and thickness $d_2$, maintaining a variable air-gap $d_1$ above the ground plane, (see Fig.1).

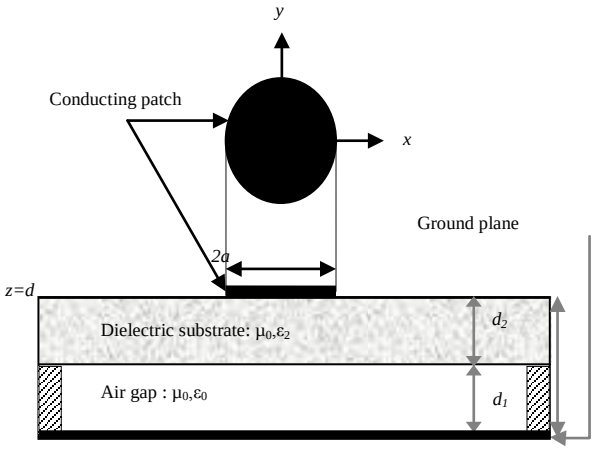


Fig. 1. Tunable circular disk microstrip structure.

All the dielectric materials are assumed to be nonmagnetic with permeability $\mu_0$. To simplify the analysis, the antenna feed will not be considered.

In this work, training and test sets are generated using the spectral domain approach [15]. For this reason, we give in this section some details about the application of the spectral approach to the calculation of resonant frequency, bandwidth and of the circular microstrip patch antenna with single layer. Our goal consists in taking into account the air gap layer in the structure shown in Fig. 1, without adding a supplementary complexity to the problem. Using electromagnetic knowledge, the thickness $d_2$, of the substrate and a variable air gap $d_1$ above the ground plane the relative permittivity $\varepsilon_r$ of the substrate are replaced by effective parameters using the following equations [16]:

$$\varepsilon_{re} = \frac{\varepsilon_r.(d_1 + d_2)}{(d_1.\varepsilon_r + d_2)} \tag{1}$$

$$d = d_2 + d_1 \tag{2}$$

The transverse fields inside the dielectric layer can be obtained via the inverse vector Hankel transforms as [21, 23-25]

$$\begin{aligned}\mathbf{E}(\rho,\phi,z) &= \begin{bmatrix} E_\rho(\rho,\phi,z) \\ E_\phi(\rho,\phi,z) \end{bmatrix} \\ &= \sum_{n=-\infty}^{n=+\infty} e^{in\phi} \int_0^\infty k_\rho dk_\rho \, \overline{\mathbf{H}}_n(\rho k_\rho).\mathbf{e}_n(k_\rho,z)\end{aligned} \tag{3}$$

$$\begin{aligned}\mathbf{H}(\rho,\phi,z) &= \begin{bmatrix} H_\phi(\rho,\phi,z) \\ -H_\rho(\rho,\phi,z) \end{bmatrix} \\ &= \sum_{n=-\infty}^{n=+\infty} e^{in\phi} \int_0^\infty k_\rho dk_\rho \, \overline{\mathbf{H}}_n(\rho k_\rho).\mathbf{h}_n(k_\rho,z)\end{aligned} \tag{4}$$

$$\overline{\mathbf{H}}_n(\rho k_\rho) = \begin{bmatrix} J_n'(\rho k_\rho) & -\dfrac{in}{\rho k_\rho} J_n(\rho k_\rho) \\ \dfrac{in}{\rho k_\rho} J_n(\rho k_\rho) & J_n'(\rho k_\rho) \end{bmatrix} \tag{5}$$

In Eq. (5), $\overline{\mathbf{H}}_n(\rho k_\rho)$ is the kernel of the vector Hankel transform (VHT) [15, 21-25], $J_n(.)$ is the Bessel function of the first kind of order $n$, and the prime denotes differentiation with respect to the

argument. The dagger implies conjugate transpose.

The relationship which relates the current on the conducting patch to the tangential electric field in the corresponding interface:

$$\mathbf{e}_n(k_\rho, z) = \overline{\mathbf{G}}(k_\rho).\mathbf{K}_n(k_\rho) \tag{6}$$

Where $\overline{\mathbf{G}}(k_\rho)$ dyadic Green's function in the vector Hankel transform domain [15, 22]. Note that in the vector Hankel transform domain, the dyadic Green's function is diagonal and it is independent of the geometry of the radiating patch.

Note that, the tensor of Green for the considered structure can be easily determined. The tangential electric field is null on the conducting patch, which leads to an integral equation. To solve the integral equation, we apply the procedure of Galerkin which consists in developing the unknown distribution of the current on the circular patch is expanded into a series of basis functions [15, 21-25]. The basis functions chosen in this article for approximating the current density on the circular patch are obtained from the model of the cavity. Boundary conditions require that the transverse components of the electric field vanish on the perfectly conducting disk and the current vanishes off the disk, to give the following set of vector dual integral equations:

$$\mathbf{E}_n(\rho, z) = \int_0^{+\infty} dk_\rho k_\rho \, \overline{\mathbf{H}}_n(k_\rho \rho). \\ \overline{\mathbf{G}}(k_\rho).\mathbf{k_n}(k_\rho) = \mathbf{0}, \qquad \rho < a \tag{7}$$

$$\mathbf{K}_n(\rho) = \int_0^{+\infty} dk_\rho k_\rho \, \overline{\mathbf{H}}_n(k_\rho \rho). \\ \mathbf{k}_n(k_\rho) = \mathbf{0}, \qquad \rho > a \tag{8}$$

The use of the method of the moments in the spectral domain allows the resolution of the system of dual integral equations. The current on the disk is expressed in the form of a series of basis functions as follows:

$$\mathbf{K}_n(\rho) = \sum_{p=1}^{P} a_{np} \, \mathbf{\Psi}_{np}(\rho) + \sum_{q=1}^{Q} b_{nq} \, \mathbf{\Phi}_{nq}(\rho) \tag{9}$$

P and Q correspond to the number of basis functions of $\mathbf{\Psi}_{np}(\rho)$ and $\mathbf{\Phi}_{nq}(\rho)$, respectively, $a_{np}$ and $b_{nq}$ are the mode expansion coefficients to be sought. The corresponding VHT of the current is given by

$$\mathbf{K}_n(\rho) = \sum_{p=1}^{P} a_{np} \, \mathbf{\Psi}_{np}(\rho) + \sum_{q=1}^{Q} b_{nq} \, \mathbf{\Phi}_{nq}(\rho) \tag{10}$$

Substitute the current expansion (10) into (7). Next, multiplying the resulting equation by $\rho \mathbf{\Psi}^{+}_{nk}(\rho)$ (k=1,2..., P) and by $\rho \mathbf{\Phi}^{+}_{nl}(\rho)$ (l=1,2...,Q), and while integrating from 0 to a, and using the Parseval's theorem for vector Hankel transform [15], we obtain a system of linear $P+Q$ algebraic equations for each mode n which can be written in the matrix form:

$$\overline{\mathbf{Z}}_n \, . \mathbf{C}_n = \mathbf{0} \tag{11}$$

where:

$$\overline{\mathbf{Z}}_n = \begin{bmatrix} (\overline{\mathbf{Z}}_n{}^{\mathbf{\Psi\Psi}}{}_n)_{P\times P} & (\overline{\mathbf{Z}}_n{}^{\mathbf{\Psi\Phi}})_{P\times Q} \\ (\overline{\mathbf{Z}}_n{}^{\mathbf{\Phi\Psi}}{}_n)_{Q\times P} & (\overline{\mathbf{Z}}_n{}^{\mathbf{\Phi\Phi}}{}_n)_{Q\times Q} \end{bmatrix}, \\ \mathbf{C}_n = \begin{bmatrix} (\mathbf{a}_n)_{p\times 1} \\ (\mathbf{b}_n)_{q\times 1} \end{bmatrix} \tag{12}$$

Each element of the submatrices is given by:

$$\overline{\mathbf{Z}}_n{}^{\mathbf{VW}}(i, j) = \int_0^{+\infty} dk\rho \, \mathbf{V}^{+}_{ni}(k_\rho).\overline{\mathbf{G}}(k_\rho).\mathbf{W}_{nj}(k_\rho) \tag{13}$$

where **V** and **W** represent either **Ψ** or **Φ**. For every value of the integer n, the system of linear equations (11) has non-trivial solutions when

$$\det\left[\overline{\mathbf{Z}}_n(\omega)\right] = 0 \tag{14}$$

This equation (14) is called characteristic equation of the structure (figure. 1). For the search of the complex roots of this equation, the method of Müller is used. It requires three initial guesses which must be close if possible to the sought solution to ensure a fast convergence.

Generally the real part ($f_r$) of the solution represents the resonant frequency of the structure, the imaginary part ($f_i$) indicates the losses of energy per radiation and the ratio ($2f_i/ f_r$) gives the band-width ($BW$) and the quantities Q=($f_r$/2 $f_i$) stands for

the quality factor [15].

# 3 Artificial Neural Networks

The ANN represents a promising modeling technique, especially for data sets having nonlinear relationships that are frequently encountered in engineering [1, 26-28]. In the course of developing an ANN model, the architecture of the neural network and the learning algorithm are the two most important factors. ANNs have many structures and architectures [1, 26]. The class of the ANN and/or the architecture selected for a particular model implementation depends on the problem to be solved. After several experiments using different architectures coupled with different learning algorithms, in this paper, the MLP neural-network architecture is used in the calculation of the resonant frequency and bandwidth of circular microstrip antenna.

## 3.1 Multilayer Perceptron (MLP) networks

Multilayer perceptrons (MLPs) [28], which are among the simplest and therefore most commonly used neural network architectures, have been adapted for the calculation of the resonant frequency. MLPs can be trained with the use of many different algorithms. In this work, the standard back-propagation algorithm has been used for training MLP.

As shown in Fig. 2, the MLP consists of an input layer, one or more hidden layers, and an output layer. Neurons in the input layer only act as buffers for distributing the input signals $x_i$ to neurons in the hidden layer. Each neuron in the hidden layer sums its input signals $x_i$ after weighting them with the strengths of the respective connections $w_{ji}$ from the input layer and computes its output $y_j$ as a function f of the sum, namely

$$y_j = f\left(\sum w_{ji} x_i\right) \qquad (15)$$

Where f can be a simple threshold function or a sigmoid or hyperbolic tangent function [28]. The output of neurons in the output layer is computed similarly.

Training of a network is accomplished through adjustment of the weights to give the desired response via the learning algorithms. An appropriate structure may still fail to give a better model unless the structure is trained by a suitable learning algorithm.

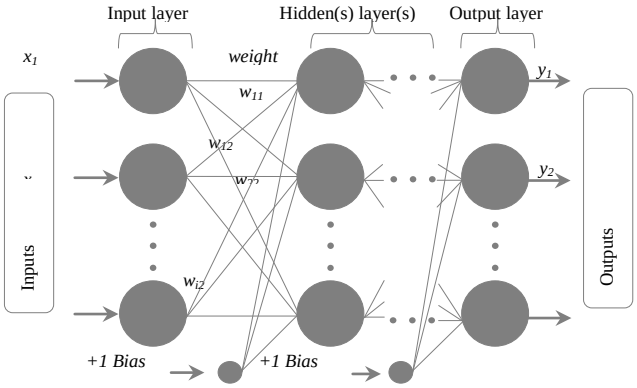


Fig. 2. General form of multilayered perceptrons.

A learning algorithm gives the change $\Delta w_{ji}$ (k) in the weight of a connection between neurons *i* and *j* at time *k*. The weights are then updated according to the formula

$$w_{ji}(k+1) = w_{ji}(k) + \Delta w_{ji}(k+1) \qquad (16)$$

In this work, Multilayer Perceptron (MLP) networks are used in ANN models. The structures of these ANNs are described briefly below.

## 3.2 Structures of the Neural Networks

In this work, Multilayer Perceptron (MLP) network is used in ANN model. MLP model is trained with almost all network learning algorithms. Hyperbolic tangent sigmoid and linear transfer functions were used in MLP training. The train and test data of the ANN were obtained from calculated with spectral model and a computer program using formulae given in Section 2. The data are in a matrix form consisting inputs and target values and arranged according to the definitions of the problems. Using [1, 28], two are generated for learning and testing the neural model. The different network input and output parameters are shown in Figure 3. As it is shown in this figure, the EM knowledge in form of empirical functions, given by (1)-(4) for the case of air gap structure, is used to preprocess the ANN model inputs. Some strategies are adopted to reduce time of training and ameliorate the ANN model accuracy, such as preprocessing of inputs and output, randomizing the distribution of the learning data [1, 26-29], and resampling with a smaller

discretization step in the part of input space corresponding to an unacceptably high error (small antenna parameters give large variation in the resonant frequency).

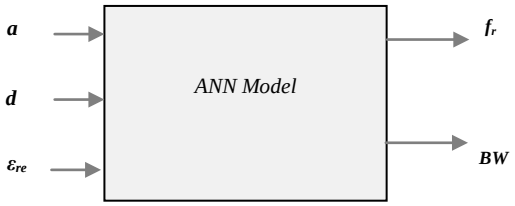


Fig. 3. Neural model for predicting the both, resonant frequency, and bandwidth of tunable circular microstrip antenna with effective parameters.

The ANN model developed here was trained with 1035 samples and tested with 345 samples. which has a configuration of 3 input neurons, 8 and 6 neurons in 2 hidden layers, and 2 outputs neurons with learning rate =0.6, goal = 0.0001, was trained for 2000 epochs. Hyperbolic tangent sigmoid and linear transfer functions were used in MLP training. The CPU time taken by the spectral domain approach to give the resonant frequency for each input set is more than half a minute; it depends on three initial values used in Muller's algorithm for root seeking of the characteristic equation. All of the results presented in the paper were obtained on a Pentium IV computer with a 2.2-GHz processor and a total RAM memory of 2 GB.

# 4 Numerical Results and Discussion

Although the full-wave analysis (moment-method analysis) presented in section2, can give results for several resonant modes [14, 15], only results for the TM11 mode are presented in this study. Since this mode is widely used in microstrip antenna applications. The neural model proposed here can also be easily adapted to determine the resonant frequency of a circular patch for higher order mode. This is done by generating, via the moment-method codes, a new data base formed by the resonant frequencies of this higher order mode instead of using the old data base.

## 4.1 Convergence and Comparison of Numerical Results

In order to confirm the computation accuracy of the neurospectral method, our results are compared with experimental and recent theoretical data [14, 30-31]. Experimental and numerical evaluations have been performed with a patch for different radius $a$, printed on single substrate ($d_1$=0) with relative permittivity $\varepsilon_r$=2.43 and thickness $d_2$=0.49mm. The Table 1 summarizes our computed resonant frequencies and those obtained for $TM^{11}$ mode via spectral domain formulation [14, 30-31]. The comparisons show a good agreement between our results and those of literature [14, 30-31].

Tab. 1. Theoretical and experimental values of the resonant frequency for the fundamonatl mode of circular microstrip antennas without air gap. $d_1$=0, $\varepsilon_r$= 2.43, $d_2$ = 0.49.

| a (mm) | a/h | Experiment (GHz) [14] | Computed (GHz) | | | |
|---|---|---|---|---|---|---|
| | | | *[14]* | *[30]* | *[31]* | *Present* |
| 1.969 | 4.02 | 25.60 | 5.30 | 5.92 | 25.4 | 25.66 |
| 3.959 | 8.08 | 13.10 | 3.30 | 3.55 | 13.3 | 13.26 |
| 5.889 | 12.02 | 8.960 | 9.13 | 9.25 | 9.20 | 9.020 |
| 8.001 | 16.33 | 6.810 | 6.80 | 6.87 | --- | 6.816 |
| 9.961 | 20.33 | 5.470 | 5.49 | 5.54 | 5.60 | 5.504 |

In order to check the accuracy of the neurospectral method for two-layered case, our results are compared with an experimental and theoretical values presented in the previous work [30].

Tab. 2. Comparison of measured and calculated frequencies for a circular microstrip patch with different thickness of air gap $d_1$, $a$ = 50 mm, $\varepsilon_r$= 2.32, $d_2$ = 1.5748 mm.

| Resonant frequency $f_r^{11}$ (GHz), Bandwidth $BW$ (%) | | | | | | |
|---|---|---|---|---|---|---|
| $d_1$ (mm) | Measured [30] | | Calculated [30] | | Our calculation | |
| | $f_r^{11}$ (GHz) | $BW$ (%) | $f_r^{11}$ (GHz) | $BW$ (%) | $f_r^{11}$ (GHz) | $BW$ (%) |
| 0.5 | 1.262 | 1.632 | 1.272 | 1.457 | 1.283 | 1.537 |
| 1 | 1.368 | 2.018 | 1.339 | 1.954 | 1.365 | 2.075 |
| 2 | 1.462 | 3.122 | 1.398 | 2.911 | 1.437 | 3.082 |
| 3 | 1.50 | 4.208 | 1.417 | 3.848 | 1.465 | 4.041 |
| 4 | 1.530 | 4.50 | 1.420 | 4.778 | 1.475 | 4.882 |

In Table 2, our calculated resonant frequencies and bandwidth are compared with measured results [30], for the tunable circular microstrip patch shown in Figure. 1. The agreement between the calculated and measured results is good for different values of air gap separation.

## 4.2 Air gap tuning effect on the resonance characteristics of a circular microstrip antenna

The effect of air gaps in between substrate and ground plane are depicted in Fig. 4 and Table 2. The resonant frequency increases with the increase of air gap is seen from the Fig. 4. So, antenna tuning is

possible by introducing the air gap without changing the antenna parameters.

It is observed that when the air separation grows, the resonant frequency increases rapidly until achieving a maximum operating frequency at a definite air separation $d_{1fmax}$.

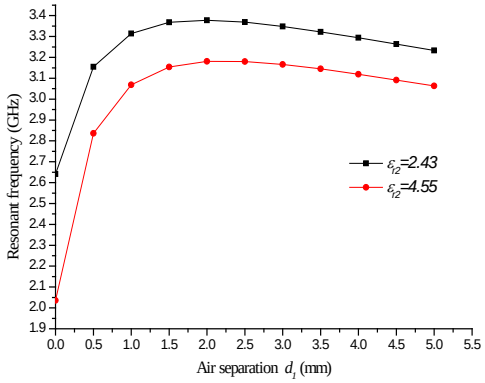


Fig. 4. Resonant frequency versus the air separation, for circular microstrip antenna for two dielectric constant; $\varepsilon_{r2}$=2.65; $\varepsilon_{r2}$=4.55, and $a$=20mm, $d_2$=1mm.

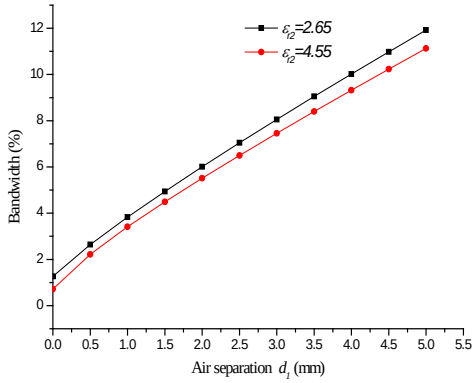


Fig. 5. Bandwidth versus the air separation, for circular microstrip antenna for two dielectric constant; $\varepsilon_{r2}$=2.65; $\varepsilon_{r2}$=4.55, and $a$=20mm, $d_2$=1mm.

Note that the effect of the air gap is more pronounced for small values of $d_1$ show "Fig. 4". When the air separation exceeds $d_{1fmax}$, increasing the air gap width will decrease slowly the resonant frequency.

Extreme care should be taken when designing an antenna with thin air gap; since small uncertainty in adjusting $d_1$ can result in an important detuning of the frequency. Fig. 5, illustrates the effect of the air separation d1 on the bandwidth. It is seen that the bandwidth increases monotonically with increasing the air separation, partly due to the increase in the total height of the dielectric medium ($d_1$+ $d_2$) and partly to the decrease in the effective permittivity of the medium under the patch.

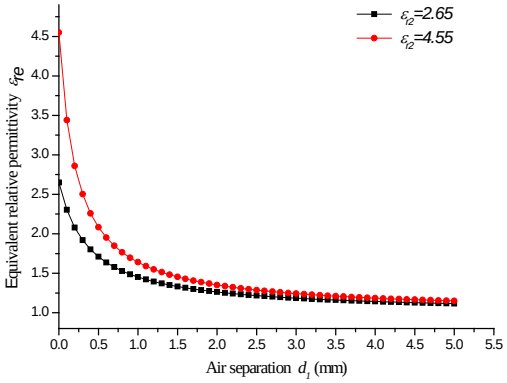


Fig. 6. Equivalent relative permittivity versus air separation for the structures studied in Figure 2.

We show in Figure.6 the equivalent relative permittivity of the composite two-layer structure, computed from [1], Equation (1), versus air separation for the structures considered in Figure. 4. It is seen that when $d_1$ increases, $\varepsilon_{req}$ decreases rapidly. This observation can well justify the very fast increase in the resonant frequency shown in Fig. 4. These behaviors agree with those discovered theoretically for resonant frequency and bandwidth of circular patch antenna [15, 30].

## 5 Conclusion

The neurospectral method presented in this work has been found to possess high accuracy and require no complicated mathematical functions. The neurospectral method is found to be well-suited for the development of fast and accurate CAD algorithms due to the improved accuracy achieved within small computational time. It take only a few microseconds to produce the resonant frequency and bandwidth after training .Computations show that the air separation can be adjusted to have the maximum operating frequency of the microstrip antenna. The half-power bandwidth, on the other hand, increases monotonically with increasing the air gap width. Extreme care should be taken when designing a microstrip antenna with thin air gap; since small uncertainty in adjusting the air separation can result in an important detuning of the frequency. The full wave analysis presented here can be used as a basic tool for the study of other patch shapes. Finally, we expect that the neural model will find wide applications in CAD of

microstrip antennas due to the improved accuracy achieved within small computational time.

## References


[1] Y. Tighilt, F. Bouttout, and A. Khellaf, "Modeling and design of printed antennas Using neural networks", Int J RF and Microwave CAE., Vol. 21, pp.228–233, 2011.

[2] V. T. Vandana, Pramod Singhal, "Microstrip Antenna Design Using Artificial Neural Networks" Int J RF and Microwave CAE 20: 76–86, 2010.

[3] D. Vijay, Lakshman M Srinivas V, Vani Ch Yuriy G, Tayfun O, "Sensitivity Driven Artificial Neural Network Correction Models for RF/Microwave Devices" Int J RF and Microwave CAE., Vol. 22, pp.30–40, 2012.

[4] Siakavara K., "Artificial neural network based design of a three-layered microstrip circular ring antenna with specified multi-frequency operation". Neural Comput & Applic., Vol.18, pp.57–64, 2009.

[5] F. Wang, V.K. Devabhaktuni, and Q.J. Zhang, "Neural net-work structures and training algorithms for RF and micro-wave applications", Int J RF Microwave Comput Aided Eng., Vol. 9, pp. 216–240, 1999.

[6] G. Kumar, and K. P. Ray, "Broadband Microstrip Antennas"Artech House, London, 2003.

[7] G. Garg, P. Bhartia, I. Bahl and A. Ittipiboon, "Microstrip AntennaDesign Handbook," Artech House, Canton, 2001.

[8] K. F. Lee, J. S. Dahele. "Circular-disk microstrip antennas with an air gaps", IEEE Trans. Antennas Propagat., AP-32, pp. 880–884, Aug. 1984.

[9] D. Guha, "Resonant frequency of circular microstrip antennas with and without air gaps", IEEE Trans. Antennas Propag., Vol. 49, No. 1, pp. 55–59 , January 2001.

[10] T. Gunel, "Continuous hybrid approach to the modified resonant frequency calculation for circular microstrip antennas with and without air gaps", Microwave Opt Tech Lett., Vol.40, No.x, pp. 423–427, 2004.

[11] C. S. Gurel, E. Aydin, and E. Yazgan, "Computation and optimization of resonant frequency and input impedance of coax-fed circular patch microstrip antenna", Microwave Opt Technol Lett, Vol.49, No.9, pp. 2263 – 2267, September 2007.

[12] R. Kumar, P. Malathi, and Yogesh B. Thakare, "On the design of four layred circular microstrip patch antenna" Microwave Opt Technol Lett, Vol.50, No.12, pp. 3206 –3212, December 2008.

[13] R. Kumar, and P. Malathi, "Experimental investigation of resonant frequency of multilayerd rectangular and circular microstrip antennas" Microwave Opt Technol Lett, Vol.53, No.2, pp.352–356, February 2011.

[14] V. Losada, R. R. Boix, and M. Horn, "Resonant modes of circular microstrip patches in multilayered substrate," IEEE Trans. Antennas propagate., Vol. 47, No. 4, pp.488-497 Apr. 1999.

[15] T. Fortaki, D. Khedrouche, F. Bouttout and A. Benghalia, "Vector Hankel transform analysis of a tunable circular microstrip patch", Commun. Numer. Meth. Engng, Vol. 21, pp. 219–231, March 2005.

[16] A. K. Verma, and Nasimuddin, "Multilayer cavity model for microstrip rectangular and circular patch antenna" Electromagnetics, Vol.24, No.3, pp.193–217, 2004.

[17] R. K. Mishra and Patnaik, A. , "Neurospectral computation for complex resonant frequency of microstrip resonators", IEEE Microwave and Guided Wave Letters, Vol. 9, No. 9, pp. 351-353, 1999.

[18] R. K. Mishra, and Patnaik, A. , "Neurospectral computation for input impedance of rectangular microstrip antenna", Electronics Letters, Vol. 35, pp.1691-1693, 1999.

[19] R. K. Mishra and Patnaik, A. , "Designing rectangular patch antenna using the neurospectral method" IEEE Transactions on Antennas and Propagation, Vol. 51, No. 8, pp. 1914-1921, 2003.

[20] F. Bouttout, F. Benabdelaziz, A. Benghalia, D. Khedrouche, and T. Fortaki, "Uniaxially anisotropic substrate effects on resonance of rectangular microstrip patch antenna," Electron. Lett., Vol. 35, No. 4, pp. 255-256, 1999.

[21] W. C.Chew, Habashy, T. M., "The use of vector transforms in solving some electromagnetic scattering problems". IEEE Transactions on Antennas and Propagation, Vol. 7, pp. 871–879, 1986.

[22] Q. Liu, and Chew, W. C., "Curve fitting formulas for fast determination of accurate resonant frequency of circular microstrip patches," IEE Proceedings, Vol. 135, Pt. H, No. 5, pp. 289–292, 1988.

[23] F. L. Mesa, R. Marqués and M. Horno, "A general algorithm for computing the bidimensional spectral green's dyadic in multiyered complex bianisotropic media: the

equivalent boundary method", IEEE transactions Microwave Theory Tech., Vol. 39, pp. 1940–1669, 1991.
[24] A. Dreher, "A new approach dyadic green's function in spectral domain ", IEEE Trans. Antennas Propagat, Vol. 43, pp. 1297- 1302, November 1995.
[25] L. Vegni, R Ciccetti, and P. Capece, "Spectral dyadic Green's function formulation for planar integrated structures", IEEE Trans. Antennas Propagat, Vol. 36, pp. 1057–1065, Aug 1988.
[26] C. Christodoulou, and M. Georgiopoulos, "Applications of Neural Networks in Electromagnetics," Norwood, MA: Artechhouse, 2001.
[27] A. Patnaik, and R. K. Mishra, "ANN techniques in microwave engineering," IEEE Micro, vol. 1, pp. 55-60, Mar. 2000.
[28] K. Guney, and S. S. Gultekin, "A comparative study of neural networks for input resistance computation of electrically thin and thick rectangular microstrip antennas" , Journal of Communications Technology and Electronics, Vol. 52, No. 5, pp. 483-492, 2007.
[29] Z. Raida, "Modeling EM structures in the neural network toolbox of MATLAB," IEEE Antennas Propag Mag 44, 46–67, 2002.
[30] F. Benmeddour, C. Dumond, F. Benabdelaziz, and F. Bouttout, "Improving the performances of a high Tc superconducting circular microstrip antenna with multilayered configuration and anisotropic" Progress In Electromagnetics Research C, Vol. 18, 169-183, 2011.
[31] A. Motevasselian, "Spectral domain analysis of resonant charcteristics and radiation patterns of a circular disc and an annular ring microstrip antenna on uniaxial susbtrate" Progress In Electromagnetics Research M, Vol. 21, 237-251, 2011.
[32] HFSS: High Frequency Structure Simulator, Ansoft Corp, Pittsburgh, PA.